Accepted Manuscript

The Influence of the Surface Parameter Changes onto the Phonon States in Ultrathin Crystalline Films

Jovan P. Šetrajčić, Dušan I. Ilić, Stevo K. Jaćimovski

Please cite this article as: J.P. Šetrajčić, D.I. Ilić, S.K. Jaćimovski, The Influence of the Surface Parameter Changes onto the Phonon States in Ultrathin Crystalline Films, *Physica A* (2018), https://doi.org/10.1016/j.physa.2017.12.138

Highlights (for review)

Highlights

- The adapted Green's functions were used to calculate phonon spectra and states in ultrathin films.
- Boundary conditions are included through the Hamiltonian of the film-structure.
- The spectral weights of phonon Green's function have been calculated.
- The localized – surface phonon states can appear for higher values of boundary parameters.
- Surface states can have a dominant role in phonon thermodynamics and transport processes.

The Influence of the Surface Parameter Changes onto the Phonon States in Ultrathin Crystalline Films

Jovan P. Šetrajčić [1,a], Dušan I. Ilić [2,b], Stevo K. Jaćimovski [3,c]

[1] University of Novi Sad, Faculty of Sciences, Department of Physics,
Trg Dositeja Obradovića 3, 21101 Novi Sad, Vojvodina – Serbia
[2] University of Novi Sad, Faculty of Technical Sciences,
Trg Dositeja Obradovića 6, 21101 Novi Sad, Vojvodina – Serbia
[3] Academy of Criminalistic and Police Studies, Belgrade, Serbia,
Cara Dušana 196, 11080 Zemun – Belgrade, Serbia

[a] bora@df.uns.ac.rs , [b] dusilic69@uns.ac.rs, [c] jacimovskis@gmail.com

Abstract

In this paper, we have analytically investigated how the changes in boundary surface parameters influence the phonon dispersion law in ultrathin films of the simple cubic crystalline structure. Spectra of possible phonon states are analysed using the method of two-time dependent Green's functions and for the diverse combination of boundary surface parameters, this problem was presented numerically and graphically. It turns out that for certain values and combinations of parameters, displacement of dispersion branches outside of bulk zone occurs, leading to the creation of localized phonon states. This fact is of great importance for the heat removal, electrical conductivity and superconducting properties of ultrathin films.

Keywords: Phonons, ultrathin films, Green's function, boundary parameters

1 Introduction

Until recently, scientists and engineers who designed and crafted devices have had a little or nothing at all to worry about microscopic properties of materials they used. The specificities of the microscopic world have been hidden in macroscopic parameters like mobility, conductance, diffusion coefficient etc. There was not much point to understand how these quantities are calculated from the basic physical principles since there was nothing that

one could do to change them. However, with the advances in fabrication techniques and miniaturization of devices situation changed drastically: it became possible to control these parameters by engineering devices on the microscopic, or even on nanoscopic scale.

Understanding of the basic physical properties of nanostructures is the first step towards their implementation. As a result of numerous factors, nanostructures are characterized by a range of different qualities: superconductivity, transport, heat insulating, acoustic and other. Most of these factors are associated with the existence of the boundaries of the structure. The main goal in this paper was to examine how the changes in boundary surface parameters influence the phonon dispersion law in ultrathin films of the simple cubic crystalline structure, which makes the basis for the concept of phonon engineering (nanophononics) [1–5]. The great importance of phonons consists in that without them, it is almost impossible to examine and describe the acoustical characteristics, as well as thermodynamic, conductive and superconductive properties of solids. In recent years thermal properties of nanostructures have attracted a lot of attention. The influence of size effects on thermal conductivity is becoming extremely important for heat removal and device design and reliability. It is also predicted that the use of nanostructured components may increase the sensitivity of measuring instruments, which in turn leads to new experimental results.

The subject of such fundamental research is not new due to the important role of phonons in transport processes in condensed systems. Apart from our team, many other research teams [1–3,6–8] have been engaged in this. In this respect, particular emphasis should be given to the research carried out in order to examine the influence of the phonon subsystem on the properties of the graphene, epitaxially grown on metals and transition carbides, which is mandatory in order to tailor graphenes mechanical properties [9–13]. We have recently published the results of the research of phonon diffusion through ultrathin crystal films [14], where we had to use the phonon dispersion law. Due to complications with analytic, we decided to consider only "ideal" film structures. In the continuation of our research, the problem of finding phonon spectra in ultrathin crystal films with different boundary conditions was solved by another approach, and now we are presenting it here. In addition, we have justifiably sought and answered the question of why phonon states are not evenly distributed; in fact, even localized – surface states may arise.

2 Phonons in bulk crystalline samples

The Hamiltonian of phonons in crystalline structures is obtained by developing the potential energy of crystals by small atomic displacements from the equilibrium position $\vec{u}_{\vec{n}}$, where $\vec{n}$ is the vector of the crystal lattice, $\vec{n} = n_x \vec{a}_x + n_y \vec{a}_y + n_z \vec{a}_z$. Here only crystals with simplest possible crystalline structure – simple cubic, with one atom per elementary cell will be observed. Although this fact may seem like a major constraint in terms of the applicability of the described model, this is not the case; namely, according to the method of achievement statistical and dynamical equivalence between rectangular and structures with lower symmetry [5], the field of its practical application is far wider. For example, in the case of monoclinic structures, the method of equivalence is applicable with no reservations. Hamiltonian of phonon subsystem in these structures, presented in nearest neighbor approximation, can be written in the form [15,16]:

$$
\begin{aligned}
H &= \sum_{\alpha;\vec{n}} \frac{p_{\alpha;\vec{n}}^2}{2M} + \sum_{\alpha;n_x,n_y,n_z} \frac{C_\alpha}{4} \left[\left(u_{\alpha;n_x+1,n_y,n_z} - u_{\alpha;n_x,n_y,n_z} \right)^2 + \right. \\
&+ \left(u_{\alpha;n_x-1,n_y,n_z} - u_{\alpha;n_x,n_y,n_z} \right)^2 + \left(u_{\alpha;n_x,n_y+1,n_z} - u_{\alpha;n_x,n_y,n_z} \right)^2 + \\
&+ \left(u_{\alpha;n_x,n_y-1,n_z} - u_{\alpha;n_x,n_y,n_z} \right)^2 + \left(u_{\alpha;n_x,n_y,n_z+1} - u_{\alpha;n_x,n_y,n_z} \right)^2 + \\
&+ \left. \left(u_{\alpha;n_x,n_y,n_z-1} - u_{\alpha;n_x,n_y,n_z} \right)^2 \right] .
\end{aligned}
\tag{1}
$$

Here, M is the mass of an atom, $u_{\alpha;\vec{n}}$ are the small movements of atom in place $\vec{n}$ from its equilibrium position in direction α, and $\vec{p}_{\alpha;\vec{n}}$ corresponding momentum. Hooke's torsion constants are disregarded in comparison to the tension constant.

In order to find the phonon dispersion law, we will make use of the phonon two-time commutator Green's function [17]:

$$
G_{\vec{n},\vec{m}}^{\alpha}(t-t') \equiv \langle\langle u_{\alpha;\vec{n}}(t) \mid u_{\alpha;\vec{m}}(t') \rangle\rangle = \Theta(t-t') \left\langle [u_{\alpha;\vec{n}}(t), u_{\alpha;\vec{m}}(t')] \right\rangle_0
\tag{2}
$$

and corresponding equation of motion:

$$
-M\omega^2 G_{\vec{n},\vec{m}}^{\alpha}(\omega) = -\frac{i\hbar}{2\pi} \delta_{\vec{n},\vec{m}} + \frac{1}{i\hbar} \left\langle\langle [p_{\alpha;\vec{n}}, H] \mid u_{\alpha;\vec{m}} \rangle\right\rangle_\omega .
\tag{3}
$$

The next step consists of calculating the commutators in Green's function from equation (3). By applying the spatial Fourier-transformation $(\vec{n}, \vec{m} \to \vec{k})$:

$$
G_{\vec{n},\vec{m}}^{\alpha}(\omega) = \frac{1}{N} \sum_{\vec{k}} e^{-i(\vec{n}-\vec{m})\vec{k}} G_{\vec{k}}^{\alpha}(\omega) ; \quad \delta_{\vec{n},\vec{m}} = \frac{1}{N} \sum_{\vec{k}} e^{-i(\vec{n}-\vec{m})\vec{k}}
$$

3

after insignificant algebraic operation we get:

$$G_{\vec{k}}^{\alpha}(\omega) = \frac{i\hbar}{4\pi M \, \omega_{\alpha}(\vec{k})} \left[\frac{1}{\omega - \omega_{\alpha}(\vec{k})} - \frac{1}{\omega + \omega_{\alpha}(\vec{k})} \right] \, , \qquad (4)$$

where $\omega_{\alpha}(\vec{k}) = 2\Omega_{\alpha}\sqrt{\sum_{j} \sin^2 \frac{a_j k_j}{2}}$, $j \in (x, y, z)$ and $\Omega_{\alpha} = \sqrt{C_{\alpha}/M}$. Here, obviously, the poles of Green's functions are obtained when the denominator of expression in brackets equate zero. After solving this condition under $\omega \equiv \omega_{\alpha}(\vec{k})$, the phonon dispersion law is obtained in form:

$$E_{\alpha}(\vec{k}) \equiv \hbar \, \omega_{\alpha}(\vec{k}) = 2 \, E_{\alpha} \sqrt{\sin^2 \frac{a_x k_x}{2} + \sin^2 \frac{a_y k_y}{2} + \sin^2 \frac{a_z k_z}{2}} \, , \qquad (5)$$

where $E_{\alpha} = \hbar\Omega_{\alpha} = \hbar\sqrt{C_{\alpha}/M}$. To compare this equation with that for ultrathin film structures, it is convenient to rewrite it in form:

$$\mathcal{E}_{\alpha}(\vec{k}) \equiv \frac{E_{\alpha}(\vec{k})}{E_{\alpha}} = 2 \, \sqrt{\mathcal{F}(k_x k_y) + \mathcal{G}(k_z)} \quad , \qquad (6)$$

or, more simply:

$$\mathcal{E}_{xyz} = 2 \, \sqrt{\mathcal{F}_{xy} + \mathcal{G}_z} \quad , \qquad (7)$$

where:

$$\mathcal{F}_{xy} \equiv \mathcal{F}(k_x k_y) = \sin^2 \frac{a_x k_x}{2} + \sin^2 \frac{a_y k_y}{2} \; ; \; \; \mathcal{G}_z \equiv \mathcal{G}(k_z) = \sin^2 \frac{a_z k_z}{2} \, .$$
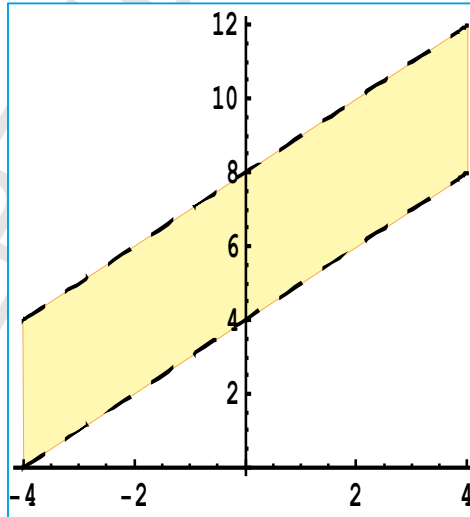

Figure 1: Phonon dispersion law for bulk structure

Figure 1 shows dependence of the square on the relative phonon energy $\mathcal{E}_{xyz}^2$ in terms of the two-dimensional function $\mathcal{F}_{xy}$ with parametric function $\mathcal{G}_z$ for the first Brillouin zone

4

of the bulk structures. The dotted lines indicate the boundaries of the bulk zone. It can be seen that within the permissible energy zone, there are as many possible energy states as the elementary particles that make up the crystal lattice. Inside a cubic crystalline sample with volume of $1cm^3$, there are $10^8 \times 10^8 \times 10^8 = 10^{24}$ atoms/molecules, so the number of possible energy states is also 10^{24}. All these energies are equally probable and their spatial distribution in the crystal is even. This is an understandable consequence of the absence of boundary conditions and deformities of the structure.

3 Formation of phonon model in ultrathin film

Ultrathin crystalline films [18–20] are crystalline structures with broken translational symmetry along direction perpendicular to the plane of film (z in our model on Fig.2), in which conditions on boundaries are different from those inside the structure.
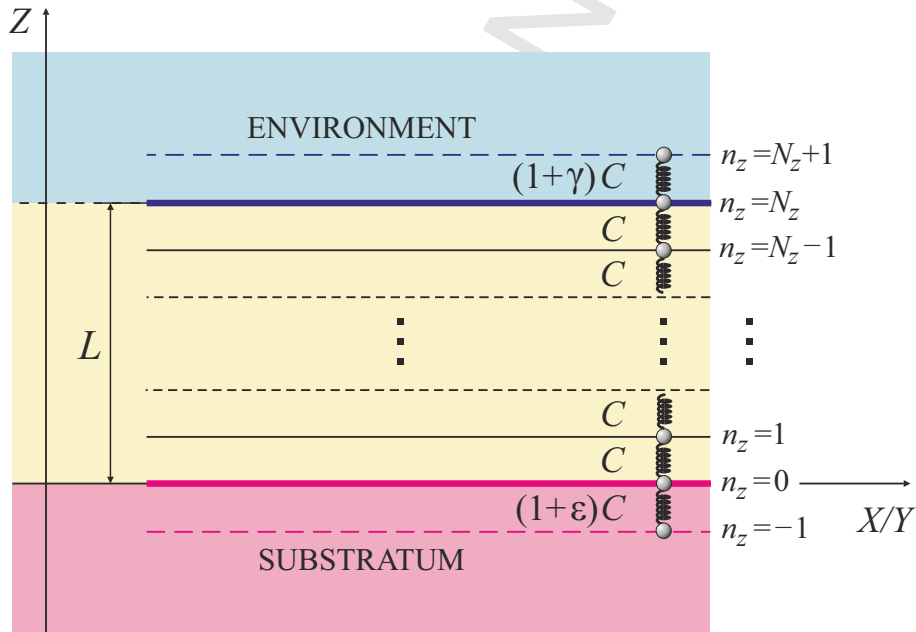

Figure 2: Ultrathin crystalline film model structure

Considering that there are no disturbances of the crystalline structure between the boundary surfaces of the film, we assume it ideal. Otherwise, if there are impurities, vacancies etc, the ultrathin film is deformed. The subject of our research in this paper is the ideal ultrathin film of simple cubic crystalline structure (see remark in first paragraph of the Section 2), whose basic crystallographic parameters are:

$$a_x = a_y = a_z = a \quad ; \quad N_{x,y} \sim 10^8 \gg N_z \sim 10 \; ;$$

$$C_{\vec{n},\vec{m}}^{\alpha,\beta} = C_{\vec{n},\vec{m}}^{\alpha,\alpha} = C_{\vec{n},\vec{n}\pm\lambda}^{\alpha} = C_{\vec{n},\vec{n}\pm\lambda} = C_{n_z,n_z\pm1} \; ;$$

$$C_{N_z,N_{z+1}} = C_{N_{z+1},N_z} = (1+\gamma)C \;, \quad C_{-1,0} = C_{0,-1} = (1+\varepsilon)C \; ; \quad \varepsilon, \gamma \in [-1, +2,5] \;,$$

where a is the lattice constant, $N_{x/y/z}$ are the numbers of atoms along x, y and $z-$directions, $C^{\alpha}-$Hooke's elastic constants and $n_z \in (0, 1, 2, \cdots, N_z)$ is the atom site counter along z direction. Considering the nature of elastic force, values of boundary parameters $\varepsilon, \gamma < -1$ are physically meaningless. On the other hand, their upper values can be arbitrary chosen, but in this research, we selected value $+2,5$ as the upper limit.

Based on the above mentioned, we can conclude the following about described model structure:

1. Carrier movement in ultrathin film is confined along z direction, while unbounded along x and y directions. That means that film structure under consideration have two boundary surfaces parallel to the XY planes (for $z = 0$ and $z = L_z = N_z a$). Along $z-$axis there are $N_z + 1$ atoms.

2. Torsion Hooke's elastic constants $C^{\alpha\beta}$ have much lower values than the straining constants C_α so that they can be ignored.

3. Despite the fact that there are no atoms belonging to the film above the upper and below the lower boundary surface of the film, we assume that interaction between boundary layers and atoms of external environment nevertheless exists through changed Hooke's forces [21–27]. Elastic constants which describe these interactions are modified with appropriate coefficients ε and γ (boundary parameters).

With respect to all these conditions and also regarding the fact that layers with $n_z \le -1$ and $n_z \ge N_z + 1$ don't exist, we have to take into account the following:

$$u_{\alpha;n_x,n_y,j} = 0 \; ; \quad -1 \ge j \;\; \wedge \;\; j \ge N_z + 1 \; ; \quad (j \notin [0, \; N_z]) \;,$$

$$C_{-1} = (1+\varepsilon) \, C \; ; \quad C_{N_z+1} = (1+\gamma) \, C \;.$$

4   Phonon states in ultrathin film

Our theoretical analysis starts from the standard form of the phonon subsystem Hamiltonian for bulk structures (1), written in the harmonic and nearest neighbors approximations and adapted to the ultrathin film model structure presented on Fig. 2:

$$
\begin{aligned}
H &= \sum_{\alpha;\vec{n}} \frac{p_{\alpha;\vec{n}}^2}{2M} + \sum_{\alpha;n_x,n_y} \sum_{n_z=-1}^{N_z+1} \frac{C_\alpha}{4} \Big[\left(u_{\alpha;n_x+1,n_y,n_z} - u_{\alpha;n_x,n_y,n_z} \right)^2 + \\
&+ \left(u_{\alpha;n_x-1,n_y,n_z} - u_{\alpha;n_x,n_y,n_z} \right)^2 + \left(u_{\alpha;n_x,n_y+1,n_z} - u_{\alpha;n_x,n_y,n_z} \right)^2 + \\
&+ \left(u_{\alpha;n_x,n_y-1,n_z} - u_{\alpha;n_x,n_y,n_z} \right)^2 + \left(u_{\alpha;n_x,n_y,n_z+1} - u_{\alpha;n_x,n_y,n_z} \right)^2 + \\
&+ \left(u_{\alpha;n_x,n_y,n_z-1} - u_{\alpha;n_x,n_y,n_z} \right)^2 \Big] \,.
\end{aligned}
\tag{8}
$$

Following the same procedure described in the previous section and by applying the partial spatial Fourier-transformation along $z-$direction, where the translational symmetry has been disrupted:

$$
G_{n_x,n_y,n_z;m_x,m_y,m_z}^{\alpha} \equiv G_{\vec{n},\vec{m}}^{\alpha}(\omega) = \frac{1}{N} \sum_{k_x,k_y} \mathrm{e}^{-ia[(n_x-m_x)k_x+(n_y-m_y)k_y]} \, G_{n_z,m_z}^{\alpha}(k_x,k_y;\omega)
\tag{9}
$$

we get the system of (N_z+1) nonhomogeneous algebraic-difference equations with the same number of undetermined Green's functions [13–25]:

$$
G_{n_z-1,m_z}^{\alpha} + \varrho_{\vec{k}}^{\alpha} \, G_{n_z,m_z}^{\alpha} + G_{n_z+1,m_z}^{\alpha} = \mathcal{K}_{n_z} \,,
\tag{10}
$$

where:

$$
\varrho_{\vec{k}}^{\alpha} = \frac{\omega^2}{\Omega_\alpha^2} - 4\sin^2\frac{ak_x}{2} - 4\sin^2\frac{ak_y}{2} - 2 \equiv \varrho \,;
\tag{11}
$$

$$
G_{n_z,m_z}^{\alpha} \equiv G_{n_z,m_z}^{\alpha}(k_x k_y;\omega) \,; \quad \Omega_\alpha^2 = \frac{C_\alpha}{M} \,; \quad \mathcal{K}_{n_z} = \frac{i\hbar}{2\pi C_\alpha}\delta_{n_z m_z} \,.
$$

The system of equations (10) can be represented in the form of the determinant:

$$
\mathcal{D}_{N_z+1}(\varrho\,;\,\varepsilon,\gamma) =
\begin{vmatrix}
\varrho-\varepsilon & 1 & 0 & 0 & \cdots & 0 & 0 & 0 & 0 \\
1 & \varrho & 1 & 0 & \cdots & 0 & 0 & 0 & 0 \\
0 & 1 & \varrho & 1 & \cdots & 0 & 0 & 0 & 0 \\
. & . & . & . & \ddots & . & . & . & . \\
0 & 0 & 0 & 0 & \cdots & 1 & \varrho & 1 & 0 \\
0 & 0 & 0 & 0 & \cdots & 0 & 1 & \varrho & 1 \\
0 & 0 & 0 & 0 & \cdots & 0 & 0 & 1 & \varrho-\gamma
\end{vmatrix}_{N_z+1} ,
\tag{12}
$$

which can be expressed through characteristic Chebyshev's polynomials of order N_z:

$$
\begin{aligned}
\mathcal{D}_{N_z+1}(\varrho;\varepsilon,\gamma) &= (\varrho-\varepsilon)(\varrho-\gamma)\,\mathcal{P}_{N_z-1}(\varrho) - (2\varrho-\varepsilon-\gamma)\,\mathcal{P}_{N_z-2}(\varrho) + \mathcal{P}_{N_z-3}(\varrho) = \\
&= \mathcal{P}_{N_z+1}(\varrho) - (\varepsilon+\gamma)\,\mathcal{P}_{N_z}(\varrho) + \varepsilon\gamma\,\mathcal{P}_{N_z-1}(\varrho) \,.
\end{aligned}
\tag{13}
$$

7

In order to find the spectra of the possible phonon energies, we need to determine the zeroes of the determinant (12), i.e. to solve the equality:

$$\mathcal{D}_{N_z+1}(\varrho;\ \varepsilon, \gamma) = 0 \ . \tag{14}$$

In that manner, we get the dispersion law of phonons in form:

$$\mathcal{E}_{\vec{k}}^{\alpha} = 2\sqrt{\sin^2 \frac{ak_x}{2} + \sin^2 \frac{ak_y}{2} + \sin^2 \frac{ak_z(\nu)}{2}} \tag{15}$$

($\nu = 1, 2, \ldots, N_z + 1$), which is almost exactly the same as the one for bulk structures (5). The difference between the two equations is, however, that quasimomentum of phonons in ultrathin films can take only discrete values in z direction, and is continual in x and y directions. The main consequence of this fact is that the phonons in ultrathin films possess upper and lower energy gaps, i.e. zone of allowed phonon energies in ultrathin films is narrower than that in bulk samples for the value of the sum of these gaps.

By applying the well-known trigonometric identity:

$$\sin^2 \alpha = \frac{1}{2} \left(1 - \cos 2\alpha\right)$$

relation (11) can be rewritten in the following form:

$$\varrho = \frac{\omega^2}{\Omega_\alpha^2} - 6 + 2 \left(\cos ak_x + \cos ak_y\right) \ . \tag{16}$$

By introducing the labels:

$$\frac{\omega^2}{\Omega_\alpha^2} - 6 \equiv \mathcal{E}_\nu^2 \qquad \text{and} \qquad 2 \left(\cos ak_x + \cos ak_y\right) \equiv \mathcal{F}_{xy} \ ,$$

from the equation (16) we get

$$\varrho = \mathcal{E}_\nu^2 + \mathcal{F}_{xy} \ . \tag{17}$$

Figures 3a and 3b shows dependance $\mathcal{E}_\nu^2 = \mathcal{E}_\nu^2 (\mathcal{F}_{xy})$ with parametric function $\mathcal{G}_\nu$ for different values of boundary parameters ε and γ for the five-layer perturbed film. Numerical calculations were carried out with the help of the program that has been created by authors, based on a commercial software package "Wolfram *Mathematica*®". It can be seen that negative values of boundary parameters ε and γ reduce the energy gaps, or spread the energy zone towards bulk values. On the other hand, for positive values of parameters, energy spectra is shifted towards higher energies, which means that energy gap increases, i.e. the highest energy levels are close to the upper limit of the bulk zone. Starting from

parameter values of $\gamma = +1,222$ and $\varepsilon = -1$ or vice versa, one localized phonon energy state appears, together with an increase in lower energy gap. Second localized phonon state arises approximately at $\gamma/\varepsilon = +1,3000$ and $\varepsilon/\gamma = +2,5000$.
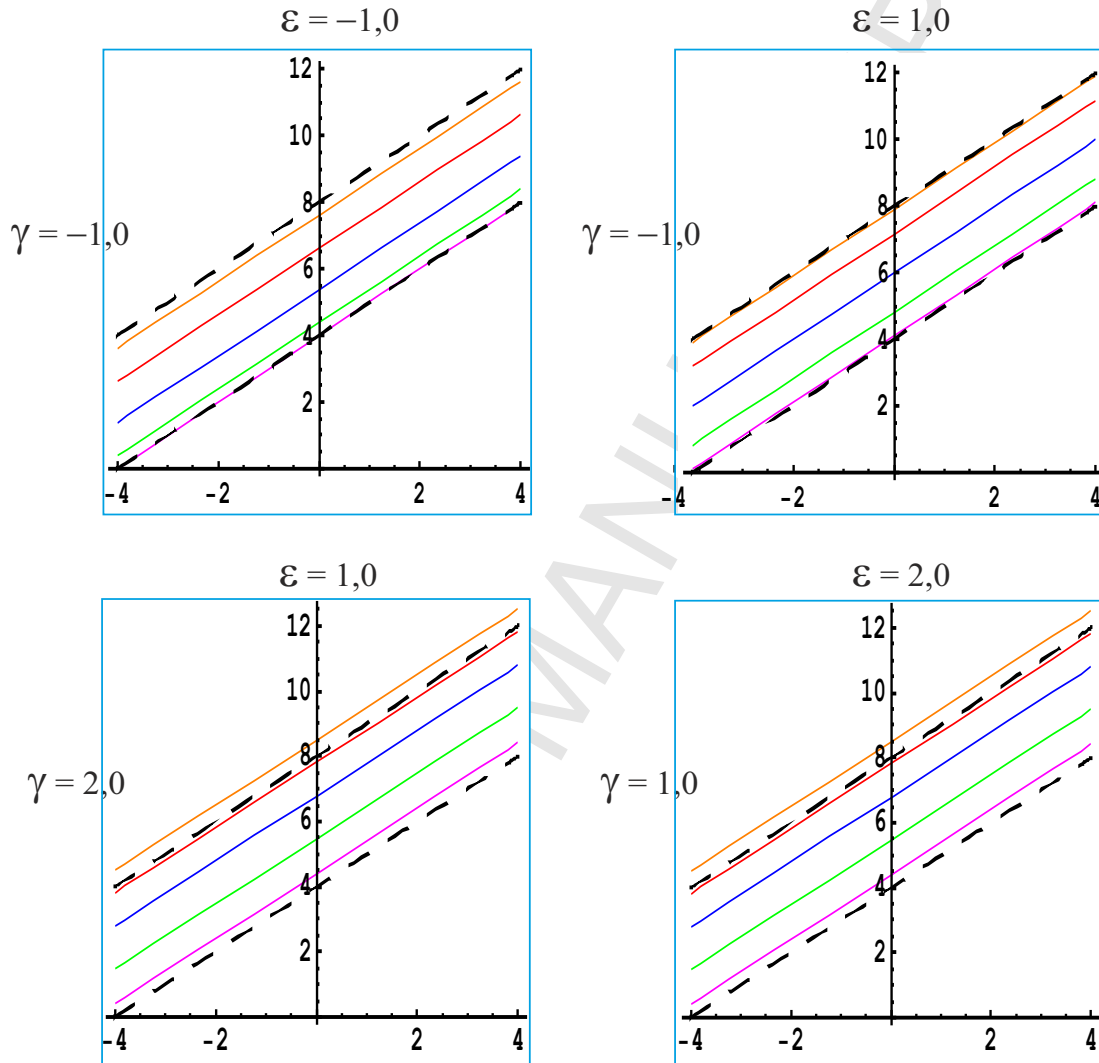

Figure 3a: Phonon dispersion law for the five-layer perturbed film with different values of boundary parameters ε and γ

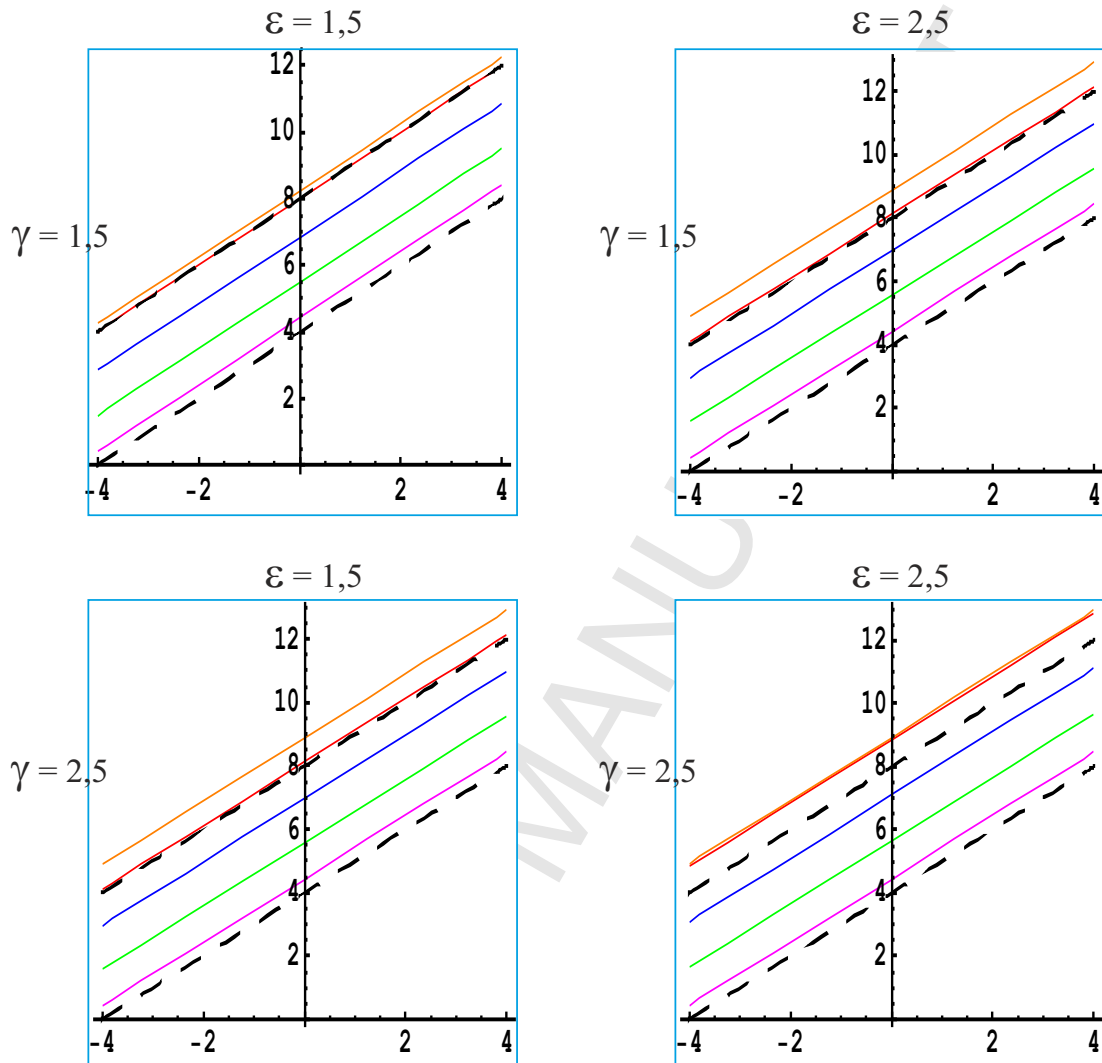Figure 3b: Phonon dispersion law for the five-layer perturbed film with different values of boundary parameters ε and γ

For a clearer overview of the critical values of boundary parameters that determine areas with zero, one or two localized states, Figure 4 is presented.
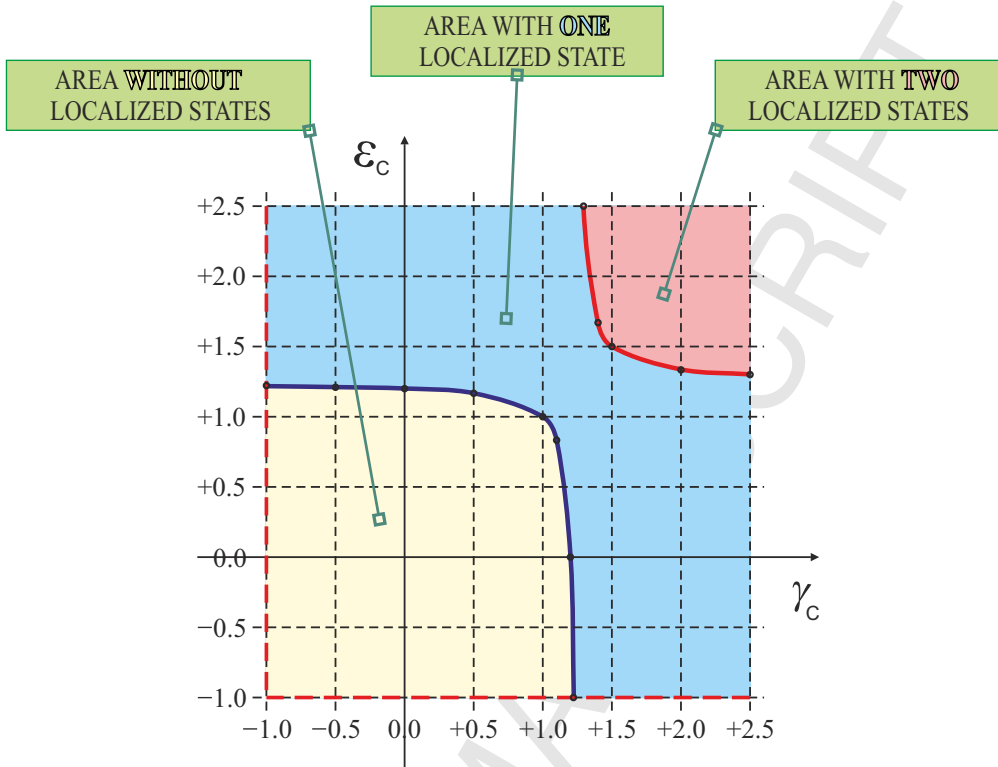
Figure 4: A graphical representation of the critical values of the boundary parameters that determine areas with zero, one or two localized states

From the obtained results, it is not possible to determine the probability of occurrence of individual phonon states (which is especially important for those physically most interesting – localized phonon states), as well as where these states are (ie, what their spatial distribution is). For the analysis of the spatial distribution of phonons, or the probability of finding the phonons with a certain energy on the individual layers of the crystalline film, it is necessary to calculate the spectral weights of individual Green's functions.

5 Spatial distribution of phonon states

The starting point for this part of research is the system of equations for Green's functions, which is most appropriately presented in the matrix form [27]:

$$\hat{\mathcal{D}}_{N+1}\tilde{\mathcal{G}}_{N+1} = \tilde{\mathcal{K}}_{N+1} \,, \tag{18}$$

11

where: $\hat{\mathcal{D}}_{N+1}-$ is the matrix corresponding to the determinant of the system $\mathcal{D}_{N_z+1}(\varrho\,;\,\varepsilon,\gamma)$ (12), and $\tilde{\mathcal{G}}_{N+1}$ and $\tilde{\mathcal{K}}_{N+1}-$ vectors that correspond to Green's functions G_{n_z,m_z}^{α} and Kronecker symbols $\mathcal{K}_{n_z}$ from equation (11):

$$
\tilde{\mathcal{G}}_{N+1} = \begin{pmatrix} G_{0,m_z} \\ G_{1,m_z} \\ \cdot \\ \cdot \\ \cdot \\ G_{n_z,m_z}\cdot \\ \cdot \\ \cdot \\ G_{N,m_z} \end{pmatrix} \quad ; \qquad \tilde{\mathcal{K}}_{N+1} = \frac{i\hbar}{2\pi C_\alpha} \begin{pmatrix} \delta_{0,m_z} \\ \delta_{1,m_z} \\ \cdot \\ \cdot \\ \cdot \\ \delta_{n_z,m_z}\cdot \\ \cdot \\ \cdot \\ \delta_{N,m_z} \end{pmatrix} .
$$

By utilizing the matrix inverse to $\hat{\mathcal{D}}_{N+1}$ from the left hand side on equation (18), we get:

$$
\tilde{\mathcal{G}}_{N+1} = \hat{\mathcal{D}}_{N+1}^{-1}\,\tilde{\mathcal{K}}_{N+1} . \tag{19}
$$

Considering that the inverse matrix $\hat{\mathcal{D}}_{N+1}^{-1}$ can be represented by an adjugated matrix whose elements D_{ik} are the cofactors of elements d_{ik} of the direct matrix [17,18], it follows $(\mathcal{D}_{N_z+1}(\varrho\,;\,\varepsilon,\gamma) \equiv \mathcal{D}_{N_z+1})$:

$$
G_{n_z,m_z} = \frac{1}{\mathcal{D}_{N_z+1}} \sum_q D_{n_z,q} K_{q,m_z} = \frac{1}{\mathcal{D}_{N_z+1}} \frac{i\hbar}{2\pi C_\alpha} \sum_q D_{n_z,q} \delta_{q,m_z} = \frac{i\hbar}{2\pi C_\alpha} \frac{D_{n_z,m_z}}{\mathcal{D}_{N_z+1}} . \tag{20}
$$

Cofactors D_{n_z,m_z} can be calculated from the determinant of the system (12).

Since for the equilibrium processes in the system only the diagonal Green's functions $G_{n_z;n_z} \equiv G_{n_z}$ are important, the calculation of the cofactors $D_{n_z,m_z} \equiv D_{n_z}$ is considerably simplified. It turns out that they are equal to the product of two auxiliary determinants:

$$
D_{n_z} = B_{n_z} B_{N-n_z} , \tag{21}
$$

where: $B_0 = B_{N-N} = 1$,

$$
B_{n_z}(\varrho) = \begin{vmatrix} \varrho - \varepsilon & 1 & 0 & \cdots & 0 & 0 & 0 \\ 1 & \varrho & 1 & \cdots & 0 & 0 & 0 \\ 0 & 1 & \varrho & \cdots & 0 & 0 & 0 \\ \cdot & \cdot & \cdot & \ddots & \cdot & \cdot & \cdot \\ 0 & 0 & 0 & \cdots & \varrho & 1 & 0 \\ 0 & 0 & 0 & \cdots & 1 & \varrho & 1 \\ 0 & 0 & 0 & \cdots & 0 & 1 & \varrho \end{vmatrix}_{n_z} , \tag{22}
$$

$$
B_{N-n_z}(\varrho) = \begin{vmatrix} \varrho & 1 & 0 & \cdots & 0 & 0 & 0 \\ 1 & \varrho & 1 & \cdots & 0 & 0 & 0 \\ 0 & 1 & \varrho & \cdots & 0 & 0 & 0 \\ . & . & . & \ddots & . & . & . \\ 0 & 0 & 0 & \cdots & \varrho & 1 & 0 \\ 0 & 0 & 0 & \cdots & 1 & \varrho & 1 \\ 0 & 0 & 0 & \cdots & 0 & 1 & \varrho - \gamma \end{vmatrix}_{N-n_z} . \tag{23}
$$

In general, the values of the auxiliary determinants can be calculated numerically, while the Green's functions of the perturbed ultrathin film are [28]:

$$
G_{n_z} = \frac{i\hbar}{2\pi C_\alpha} \frac{B_{n_z} B_{N-n_z}}{\mathcal{D}_{N_z+1}} . \tag{24}
$$

Since Green's functions have multiple poles (because in denominator exists polynomial $\mathcal{D}_{N_z+1}$ of order $N_z + 1$), it is necessary to carry out the process of factorization in simple poles:

$$
G_{n_z} = \frac{i\hbar}{2\pi C_\alpha} \sum_{\nu=1}^{N+1} \frac{g_{n_z;n_z}(\varrho_\nu)}{\varrho - \varrho_\nu} . \tag{25}
$$

Spectral weights $g_{n_z;n_z}(\varrho_\nu) \equiv g_{n_z}^\nu$ of phonon Green's function then can be expressed in form:

$$
g_{n_z}^\nu = \frac{B_{n_z}(\varrho_\nu) B_{N-n_z}(\varrho_\nu)}{\left. \dfrac{d}{d\varrho} D_{N_z+1}(\varrho) \right|_{\varrho=\varrho(\nu)}} . \tag{26}
$$

The spectral weights of Green's function give the probability distribution of finding phonons with certain energy on the individual layers of the crystalline film. In the tables 1 and 2 and on the figures 5a and 5b, the values of the reduced phonon energies and corresponding spectral functions (spatial distribution of probabilities) in the five-layer perturbed film are presented. As with the determination of phonon states, the spectral weights for the given phonon energies are calculated numerically. It should be noted that only characteristic examples are selected and shown here. The figures show the spatial distribution of the probability of finding phonons with the corresponding energies on the individual layers of the crystalline film, while in the bottom line, summarized graphics for all energy distributions are shown. Energies with values located outside the bulk zone (localized phonon states), as well as the highest probability values per film layers, are highlighted in tables.

13

Reduced relative ENERGY	$\varepsilon = -1,0; \quad \gamma = -1,0$				
	0. plane	1. plane	2. plane	3. plane	4. plane
4,00000	0,16552	0,22174	0,22548	0,22174	0,16552
4,38197	0,16904	0,21971	0,22250	0,21971	0,16904
5,38197	0,17551	0,21585	0,21729	0,21585	0,17551
6,61803	0,18050	0,21275	0,21350	0,21275	0,18050
7,61803	0,18325	0,21100	0,21149	0,21100	0,18325

Reduced relative ENERGY	$\varepsilon = -1,0; \quad \gamma = 0,0$				
	0. plane	1. plane	2. plane	3. plane	4. plane
4,08101	0,15891	0,21140	0,21494	0,21424	0,20051
4,69028	0,16473	0,20986	0,21210	0,21171	0,20161
5,71537	0,17142	0,20799	0,20918	0,20900	0,20240
6,83083	0,17627	0,20660	0,20728	0,20719	0,20265
7,68251	0,17897	0,20582	0,20629	0,20624	0,20268

Reduced relative ENERGY	$\varepsilon = 0,0; \quad \gamma = +2,0$				
	0. plane	1. plane	2. plane	3. plane	4. plane
4,33760	0,16133	0,17099	0,17205	0,18016	0,31547
5,24263	0,17232	0,17910	0,17952	0,18354	0,28552
6,42494	0,17991	0,18450	0,18467	0,18665	0,26428
7,49592	0,18396	0,18736	0,18744	0,18863	0,25261
8,49889	0,18653	0,18919	0,18924	0,19002	**0,24501**

Table 1: The probabilities of phonon states in the five-layer perturbed film
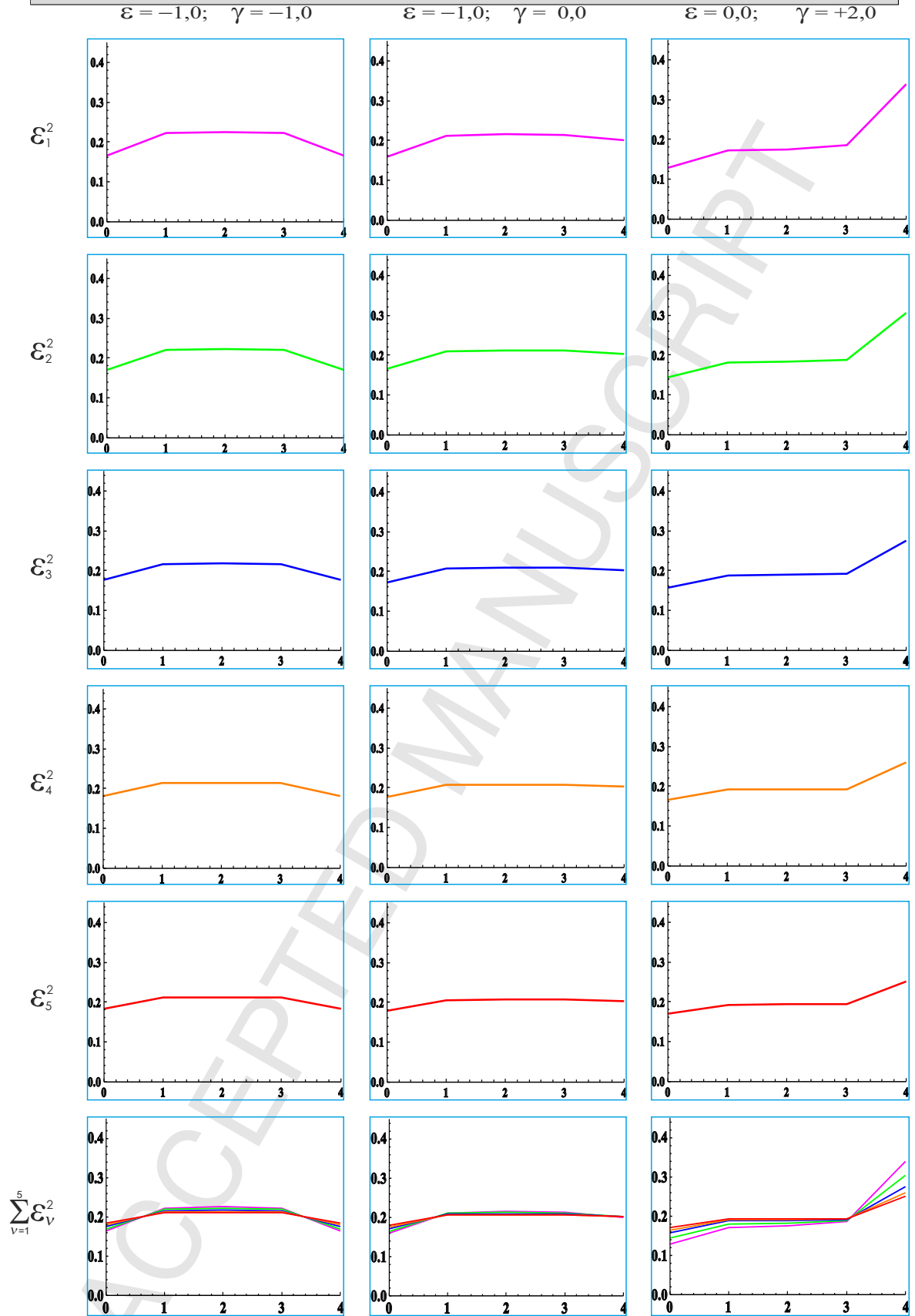
Figure 5a: A graphical representation of the probabilities of phonon states in the five-layer perturbed film

15

Reduced relative ENERGY	$\varepsilon = +2,0;\quad \gamma = -1,0$				
	0. plane	1. plane	2. plane	3. plane	4. plane
4,10475	0,33897	0,18556	0,17498	0,17142	0,12907
4,88192	0,30480	0,18819	0,18275	0,18080	0,14346
6,13706	0,27564	0,19103	0,18863	0,18770	0,15699
7,37850	0,25957	0,19282	0,19153	0,19102	0,16507
8,49778	**0,25007**	0,19393	0,19313	0,19280	0,17007

Reduced relative ENERGY	$\varepsilon = +1,5;\quad \gamma = +2,5$				
	0. plane	1. plane	2. plane	3. plane	4. plane
4,43482	0,21245	0,14861	0,14557	0,15570	0,33767
5,57165	0,21651	0,16368	0,16201	0,16626	0,29153
6,96808	0,21565	0,17287	0,17199	0,17394	0,26555
8,12420	0,21430	0,17746	0,17690	0,17807	**0,25327**
8,90126	0,21341	0,17974	0,17932	0,18018	**0,24735**

Reduced relative ENERGY	$\varepsilon = +2,5;\quad \gamma = +2,5$				
	0. plane	1. plane	2. plane	3. plane	4. plane
4,45673	0,29735	0,13792	0,12946	0,13792	0,29735
5,64922	0,26920	0,15510	0,15140	0,15510	0,26920
7,10123	0,25144	0,16628	0,16456	0,16628	0,25144
8,85078	**0,23939**	0,17402	0,17318	0,17402	**0,23939**
8,94204	**0,23892**	0,17433	0,17351	0,17433	**0,23892**

Table 2: The probabilities of phonon states in the five-layer perturbed film

16

Figure 5b: A graphical representation of the probabilities of phonon states in the five-layer perturbed film
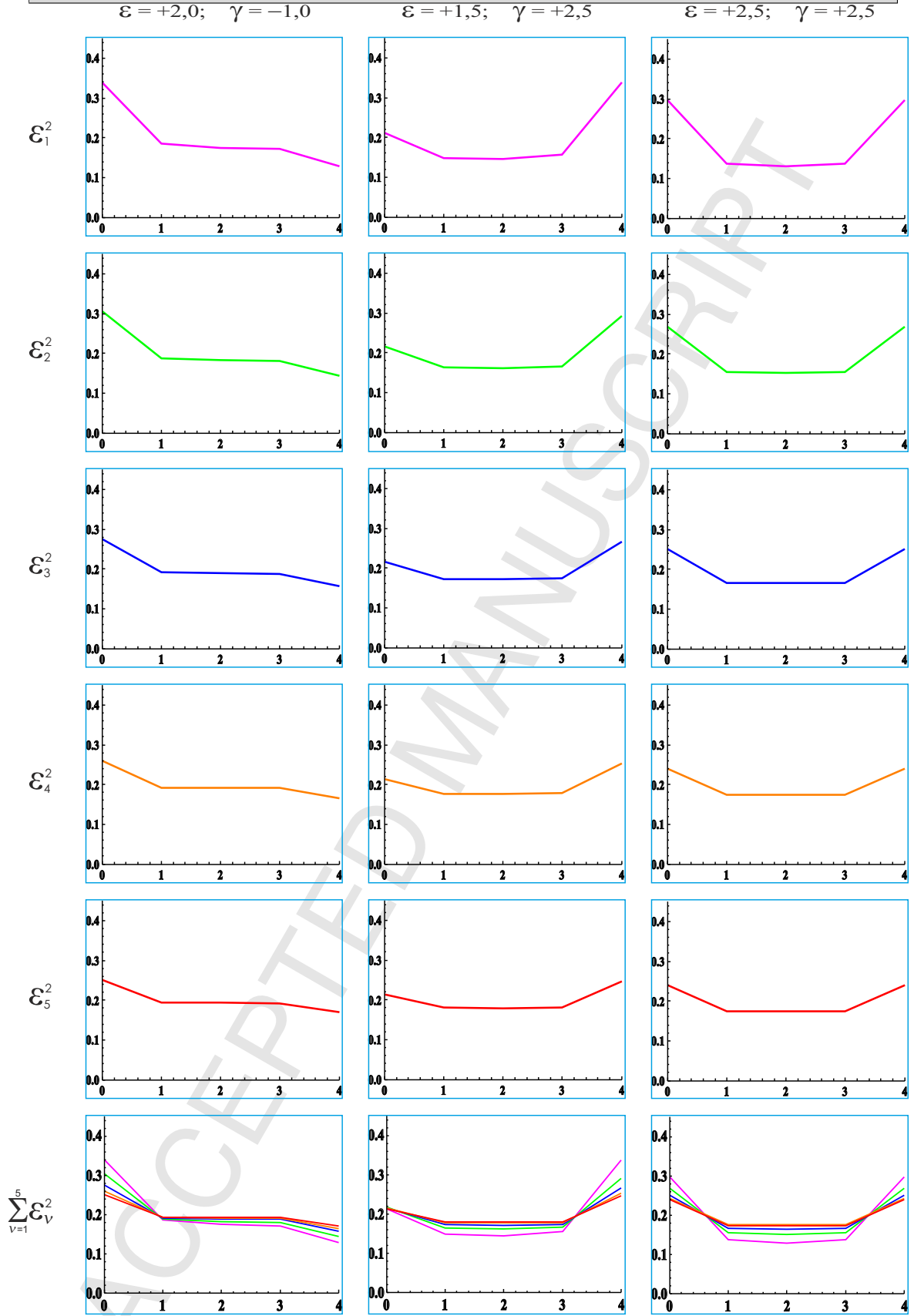
From the two left columns in Figure 5a can be seen that the probability of finding unlocalized phonon states is approximately uniformly distributed over all layers of the film. This is understandable, because the boundary conditions are poorly perturbed ($\varepsilon, \gamma \leq 1$). On the right column of Figure 5a and from the first column of Figure 5b, the greatest probability of locating precisely localized states is detected at one boundary level, when the values of the parameters are in the interval $1, 2 < \varepsilon, \gamma \leq 1, 5$. The two right columns of figure 5b show the appearance of two localized phonon states with equal probabilities of appearance on both film boundaries. The probability of their appearance is greatest at the boundary layer with a higher value of the boundary parameter. In cases where the values of the boundary parameters are the same, the probability of appearance of the localized phonon states is equal on both boundary layers. These are in fact surface states that occur for $\varepsilon, \gamma > 1, 5$ and dominate in relation to the remaining bulk phonon states.

6 Conclusions

The central topic of this paper is the description of the acoustic phonons of the optical type and phonon related effects in structures with nanoscale dimensional confinement in one spatial dimension, namely ultrathin crystalline films. It is known that acoustic phonons have considerable influence on thermal, optical and electronic properties of materials. They are heat carriers and – together with optical phonons – significantly affect the mobility of electrons in medium and high-temperature regimes. Confinement of phonons due to the size-reduction in nanostructures results in dimensional quantization of phonon branches and substantial modification of their energy spectrum, group velocity, and polarization. The concept of phonon engineering is based on these changes, in order to improve thermal and electric transport properties of the material under study. In homogeneous layers, phonon engineering can be achieved either by changes in the size or by changes in the exterior surfaces. Latter was the subject of this paper, where we have simulated different exterior environments of the ultrathin film by means of changing in Hooke's constants through different values of the boundary parameters. The results we have obtained are as follows.

In the five-layer film, there are five possible quantum phonon states. For the lesser values of the boundary parameters, which describe the interaction of the film with the substratum and the external environment, there are no localized states, but all the states

18

are within the phonon bulk zone with approximately the same distribution across all layers of the film. For higher values of boundary parameters, one $(1, 2 \leq \varepsilon, \gamma < 1, 5)$ or two $(1, 5 \leq \varepsilon, \gamma \leq 2, 5)$ localized states may occur. The analysis has shown that these are the surface phonon states, with the greatest distribution probability at the very boundary surfaces of the film (one or both). These localized states are physically particularly interesting, because their presence certainly changes the thermodynamic behavior of the phonon system in the ultrathin film. It is not difficult to conclude that due to the presence of localized phonon states, the interactions of all (quasi)particles present in this structure will have to be redefined. This means that the phonon contribution in the transport of heat, electrical conductivity and superconducting properties should be determined.

Acknowledgements

References

1. A.A. Balandin, D.L. Nika: Phononics in low-dimensional materials, *Materials Today* **15**/6, 266-275 (2012).

2. A.A. Balandin: Nanophononics: fine-tuning phonon dispersion in semiconductor nanostructures, *Moldavian Journal of the Physical Sciences* **6**/1, 1-7 (2007).

3. N. Yang, X. Xu, G. Zhang, and B. Li: Thermal transport in nanostructures, *AIP Advances* **2**, 041410 (2012).

4. J.P. Šetrajčić, S.K. Jaćimovski, and V.D. Sajfert: Phonon contribution to heat capacitance of nanolayered crystalline structures, *Modern Physics Letters* B **29**, 1550008 (2015).

5. V. Sajfert, S. Jaćimovski, D. Popov, and B. Tošić: Statistical and dynamical equivalence of different elementary cells, *Journal of Computational and Theoretical Nanoscience* **4**/3, 1-8, (2007).

6. S. Liu, X.F. Xu, R.G. Xie, G. Zhang, B.W. Li, Anomalous heat conduction and anomalous diffusion in low dimensional nanoscale systems, *Eur.Phys.J.*B **85**, 337 (2012); doi:https://doi.org/10.1140/epjb/e2012-30383-8.

7. D. Li, A.J.H. McGaughey, Phonon dynamics at surfaces and interfaces and its implications in energy transport in nanostructured materials – an opinion paper, *Nanoscale and Microscale Thermophysical Engineering* **19**/2, 166-182 (2015); doi:10.1080/15567265.2015.1035199.

8. J.B. Pendry, K.Sasihithlu, R.V. Craster: Phonon-assisted heat transfer between vacuum-separated surfaces, *Phys.Rev.*B **94**, 075414 (2016); doi:https://doi.org/10.1103/PhysRevB.94.075414

9. S.K. Jaćimovski, M. Bukurov, J.P. Šetrajčić, D.I.Raković: Phonon thermal conductivity of graphene, *Superlattices and Microstr.* **88**, 330337 (2015); doi:10.1016/j.spmi.2015.09.027.

10. A. Politano: Spectroscopic investigations of phonons in epitaxial graphene, *Crit.Rev.Solid State Mater.Sci.* **42** 99-128 (2017).

11. A. Politano, F. de Juan, G. Chiarello, H.A. Fertig: Emergence of an out-of-plane optical phonon (ZO) Kohn anomaly in quasifreestanding epitaxial graphene, *Phys.Rev.Lett.* **115** 075504 (2015); doi:10.1103/PhysRevLett.115.075504.

12. A. Al Taleb, D. Faras: Phonon dynamics of graphene on metals, *J.Phys.: Condens. Matter* **28**, 103005 (2016); doi:10.1088/0953-8984/28/10/103005.

13. A. France-Lanord, P. Soukiassian, C. Glattli, E. Wimmer: Thermal transport in supported graphene: substrate effects on collective excitations, *Phys.Rev.Applied* **7**, 034030 (2017); doi:10.1103/PhysRevApplied.7.034030.

14. J.P. Šetrajčić, S.K. Jaćimovski, and V.D. Sajfert: Diffusion of phonons through (along and across) the ultrathin crystalline films, *Physica* A **486**, 839848 (2017); doi:http://dx.doi.org/10.1016/j.physa.2017.06.003.

15. C. Kittel: Introduction to solid state physics, *Wiley*, New York 1986.

16. W. Jones and N.H. March: Theoretical solid state physics, Vol. 2, *Dover*, New York 1985.

17. G. Rickayzen: Green's functions and condensed matter, *Academic Press*, London 1980.

18. H.C. Chang, E.A. Demekhin: Complex wave dynamics on thin films, *Elsevier*, Amsterdam 2002.

19. G. Decher, J.B. Schlenoff (Eds.): Multilayer thin films – sequential assembly of nanocomposite materials, *Wiley-VCH*, Weinheim 2003.

20. S.N. Karmakar, S.K. Maiti, J. Chowdhury (Eds.): Physics of zero- and one-dimensional nanoscopic systems, *Springer-Verlag*, Berlin Heidelberg 2007.

21. M.G. Cottam, D.R. Tilley: Introduction to surface and superlattice excitations, *University Press*, Cambridge 1989.

22. S.G. Davison, M. Steslicka: Basic theory of surface states, *Clarendon*, Oxford 1996.

23. J.P. Šetrajčić, S.K. Jaćimovski, D. Raković and D.I. Ilić: Phonon spectra in crystalline nanostructures, pp. 146-151, In: Electrical and computer engineering series, N.E. Mastorakis, V.V. Kluev and Dj. Koruga, Eds.: Advances in simulation, systems theory and systems engineering, *WSEAS Press*, Singapore 2002.

24. J.P. Šetrajčić, D.Lj. Mirjanić, S.M. Vučenović, D.I. Ilić, B. Markoski, S.K. Jaćimovski, V.D. Sajfert, V.M. Zorić: Phonon contribution in thermodynamics of nano-crystalline films and wires, *Acta Physica Polonica* A **115**/4, 778-782 (2009).

25. S.K.Jaćimovki, J.P. Šetrajčić, M.S. Jaćimovski and V.V. Stojanović: Phonon contribution in thermodynamics and transport properties of ultrathin ceramic films, *Acta Phys.Pol.* A **126**/3, 811-819 (2014).

26. J.P. Šetrajčić, V.D. Sajfert, and S.K.Jaćimovski: Fundamental preferences of the phonon engineering for nanostructural samples, *Rev.Theor.Sci.* **4**/4, 353-401 (2016).

27. B.S. Tošić, J.P. Šetrajčić, R.P. Djajić and D.Lj. Mirjanić: Phonons in broken-symmetry structures, *Phys. Rev.* B **36**, 9094-9097 (1987).

28. J.P. Šetrajčić: Adequate determination of micro and macro properties of optical nano-crystals, *Opto-Electron.Rev.* **25**/4, 303-310 (2017); doi:https://doi.org/10.1016/j.opelre.2017.08.003.